Supplementary Material (ESI) for Chemical Communications

Supporting Information

Self-assembly of Cerium-based Metal-Organic Tetrahedrons for Size-Selectively Luminescent Sensing Natural Saccharides

Yang Liu, Xiao Wu, Cheng He, Yang Jiao and Chunying Duan

Contents

1. Experimental Section.

1.1 Materials and Methods. All chemicals were of reagent grade quality obtained from commercial sources and used without further purification. The elemental analyses of C, H and N were performed on a vario EL III elemental analyzer. ^{1}H NMR spectra were measured on a BRUKER 400M spectrometer. ESI mass spectra were carried out on a HPLC-Q-Tof MS spectrometer using methanol as mobile phase. Uv-*vis* spectra were measured on a HP 8453 spectrometer. The fluorescent spectra were measured on EDINBURGH FS920. The emission quantum yield of the complexes was estimated with reference to quinine sulfate (Φ_f = 0.546 in 1N sulfuric acid with excitation at 365 nm) [S1] as the standard.

$$\Phi_{unk} = \Phi_{std} \frac{(I_{unk}/A_{unk})}{(I_{std}/A_{std})} \left(\frac{\eta_{unk}}{\eta_{std}}\right)^2 \quad (1)$$

Where Φunk and Φstd are the radiative quantum yields of the sample and standard, *Iunk* and *Istd* are the integrated emission intensities of the corrected spectra for the sample and standard, *Aunk* and Astd are the absorbance of the sample and standard at the excitation wavelength, and η_{unk} and η_{std} are the indices of refraction of the sample and standard solutions, respectively.

1.2 Preparation

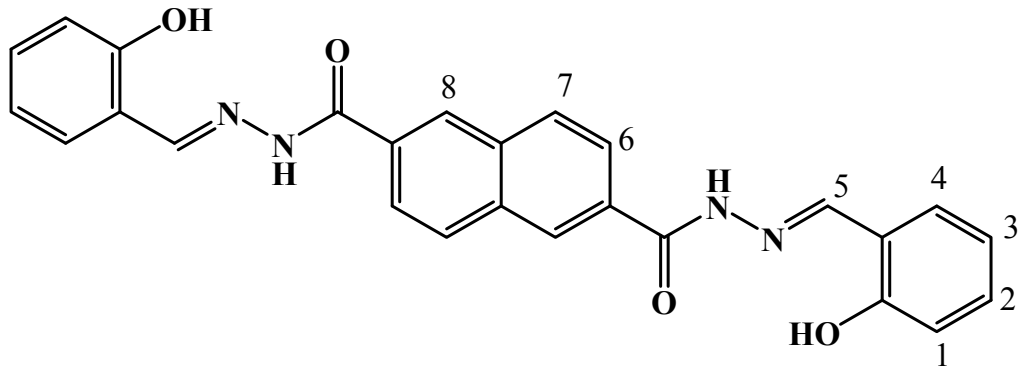

H_2L^1

2,6-naphthalene-dicarbohydrazide: A mixture solution of 80% hydrazine hydrate (40mmol, 2.50g) and dimethyl-2,6-naphthalene-dicarboxylate (4mmol, 0.86g) in methanol (20mL) was stirred over 12h. A white precipitate was formed, which was collected by filtration, washed with methanol and dried in vacuum. Yield: 0.80g, 82%.

H_2L^1: 2,6-naphthalene-dicarbohydrazide (3 mmol, 0.732g) was added to a CH_3OH solution (60 mL) containing salicylaldehyde (6.4 mmol, 0.781 g). After 5 drops of acetic acid was added, the yellow mixture was heated at boiling temperature under magnetic stirring for 24h. During the reaction, a pale yellow precipitate was formed, which was collected by filtration. Yield: 1.11g, 82%. Anal calc. for $C_{26}H_{20}N_4O_4 \cdot 2H_2O$: H 4.95, C 63.93, N 11.47%. Found: H 4.90, C 64.00, N 11.16%. ^{1}H NMR (DMSO-d_6,

ppm): 12.35(s, $2H_{NH}$), 11.26(s, $2H_{OH}$), 8.72(s, $2H_5$), 8.65(s, $2H_8$), 8.25(d, $2H_6$, J = 8.4Hz), 8.10(d, $2H_7$, J = 8.4Hz), 7.60(d, $2H_4$, J = 6.8Hz), 7.33(t, $2H_2$, J = 8.0Hz), 6.95(m, $2H_3$, $2H_1$).

TE1: A solution of $Ce(NO_3)_3 \cdot 6H_2O$ (8.4 mg, 0.02 mmol), $H_2\mathbf{L}^1$ ligand (13.6 mg, 0.03mmol) and KOH (3.4 mg, 0.06 mmol) in CH_3OH/DMF (v:v = 1:7, 8 mL) was stirred for 2h. Then the solution was left for two weeks at room temperature to give X-ray quality black block crystals. Anal calc. for $Ce_4(C_{26}H_{18}N_4O_4)_6 \cdot 4C_3H_7NO \cdot 6H_2O \cdot 2CH_3OH$: H 4.22, C 54.77, N 10.52%. Found: H 4.25, C 54.89, N 10.42 %. Yield: 65%.

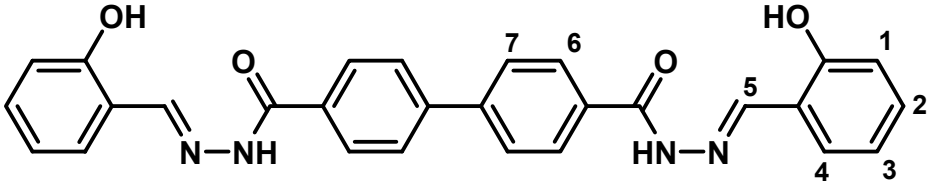

$H_2\mathbf{L}^2$

4,4'-biphenyl-dicarbohydrazide: A mixture solution of 80% hydrazine hydrate (20mmol, 1.25g) and dimethyl-4,4'-biphenyl-dicarboxylate (2mmol, 0.49g) in methanol (20mL) was stirred over 12h. A white precipitate was formed, which was collected by filtration, washed with methanol and dried in *vacuum*. Yield: 0.43g, 80%

$H_2\mathbf{L}^2$: 4,4'-biphenyl-dicarbohydrazide (3 mmol, 0.81g) was added to a CH_3OH solution (60 mL) containing salicylaldehyde (6.4 mmol, 0.78 g). After 5 drops of acetic acid was added, the yellow mixture was heated at boiling temperature under magnetic stirring for 24h. During the reaction, a pale yellow precipitate was formed, which was collected by filtration. Yield: 1.20g, 83%. Anal calc. for $C_{28}H_{22}N_4O_4 \cdot 0.5CH_3OH$: H 4.89, C 69.22, N 11.33 %. Found: H 4.95, C 68.90, N 11.25%. ^{1}H NMR (DMSO-d_6, ppm): 12.21(s, $2H_{NH}$), 11.30(s, $2H_{OH}$), 8.69(s, $2H_5$), 8.09(d, $2H_6$, J = 8.4Hz)), 7.97(d, $2H_7$, J = 8.4Hz), 7.57(d, $2H_4$, J = 6.4Hz), 7.32(t, $2H_2$, J = 8.0Hz), 6.95(m, $2H_3$, $2H_1$).

TE2: A solution of $Ce(NO_3)_3 \cdot 6H_2O$ (8.4 mg, 0.02 mmol), **$H_2\mathbf{L}^2$** ligand (14.4 mg, 0.03mmol) and KOH (3.4 mg, 0.06 mmol) in CH_3OH/DMF (v:v = 1:7, 8 mL) was stirred for 2h. Then the solution was left for two weeks at room temperature to give crystalline solid. The solid were dried vacuum. Anal calc. for $Ce_4(C_{28}H_{22}N_4O_4)_6 \cdot 2C_3H_7NO \cdot 2H_2O$: H 4.18, C 57.83, N 10.08 %. Found: H 4.25, C 58.37, N 10.32 %. Yield: 60%.

Reference

S1 G. A. Crosby and J. N. Demas, *J. Phys. Chem*. 1971, **75**, 991 – 1024.

2. Crystallography:

Intensities of **TE1** was collected on a Bruker SMART APEX CCD diffractometer with graphite-monochromated Mo-Kα (λ = 0.71073 Å) using the SMART and SAINT programs. The structures were solved by direct methods and refined on F^2 by full-matrix least-squares methods with SHELXTL *version* 5.1. Crystal data of **TE1** $C_{170}H_{156}Ce_4N_{28}O_{36}$, M = 3727.71, monoclinic, space group $P2_1/n$, black block, a = 24.009 (1), b = 37.450 (1), c = 24.065 (1) Å, β = 92.650(2)°, V = 21614 (1) Å^3, Z = 4, Dc = 1.146 g cm^{-3}, μ(Mo-Kα) = 0.891 mm^{-1}, T = 180(2) K. 31778 unique reflections [Rint = 0.1333]. Final $R1$ [with $I > 2\sigma(I)$] = 0.0849, $wR2$ (all data) = 0.1991 for 2θ = 47º. CCDC number 705880.

In the structural refinement of **TE1**, non-hydrogen atoms, except the disordered solvent molecules were refined anisotropically. Hydrogen atoms within the ligand backbones were fixed geometrically at calculated distances and allowed to ride on the parent non-hydrogen atoms, whereas no hydrogen atoms corresponding to the disordered solvent molecules were added and refined. To assist the stability of refinements, several restrains were applied: (1)Four of the six naphthalene rings, seven of the twelve benzene rings and one hydroxyl oxygen atom were disordered into two parts. Except two of the benzene rings were refined as free variables, the others were refined with the site occupancy factors (*s.o.f.*) being fixed at 0.5. (2) For all the disordered rings, the geometrical constraints of idealized regular polygons were used, the C−C bond distance of the phenyl ring being 1.39 Å and the diagonal C−C distance of the phenyl ring being 2.78 Å. (3) thermal parameters on adjacent atoms in the disordered moieties were restrained to be similar. (4) Several partially occupied solvent molecules were disordered with the *s.o.f.* being fixed at suitable value. On the checkcif report, the short interatom separations are due to the disorder of corresponding solvent molecules.

3. Figure S1 ESI-MS of **TE1** (top) and **TE2** (Bottom) in DMF/CH_3OH in present of KOH (0.1mM). The insert exhibits the measured and simulated isotopic patterns at 1097.45 (for **TE1**) and 1137.19 (for **TE2**) respectively.

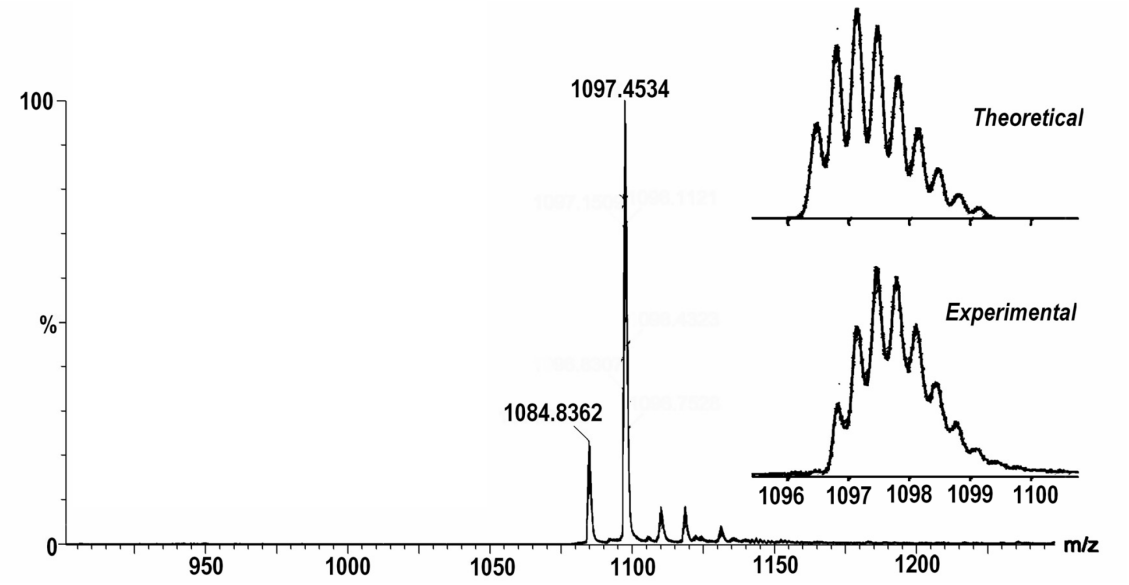

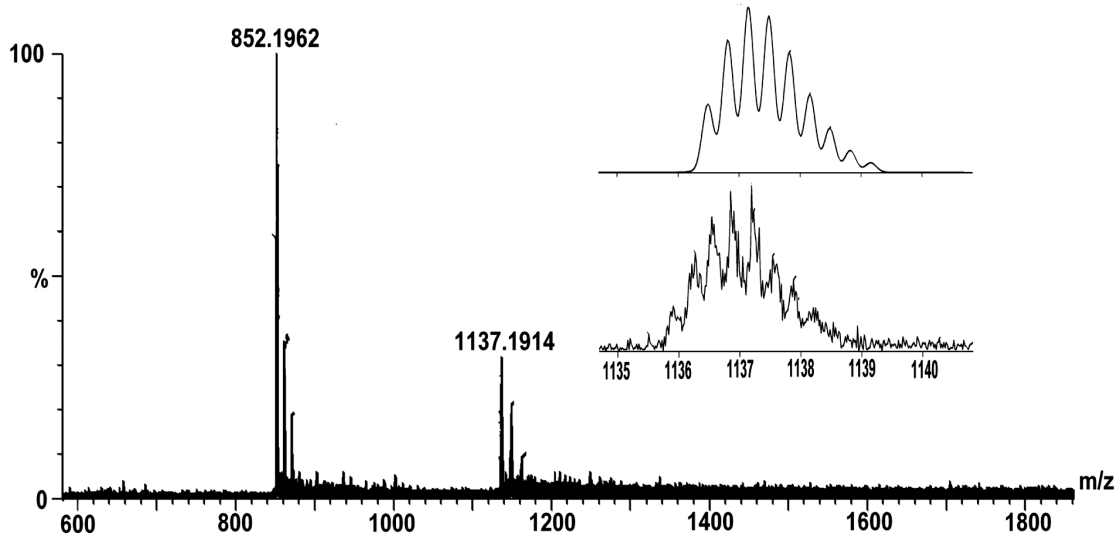

4. Figure S2 Molecular structure of the tetrahedron in **TE1,** including the disordered parts of ligands. The hydrogen atoms and solvent molecules were omitted for clarity.

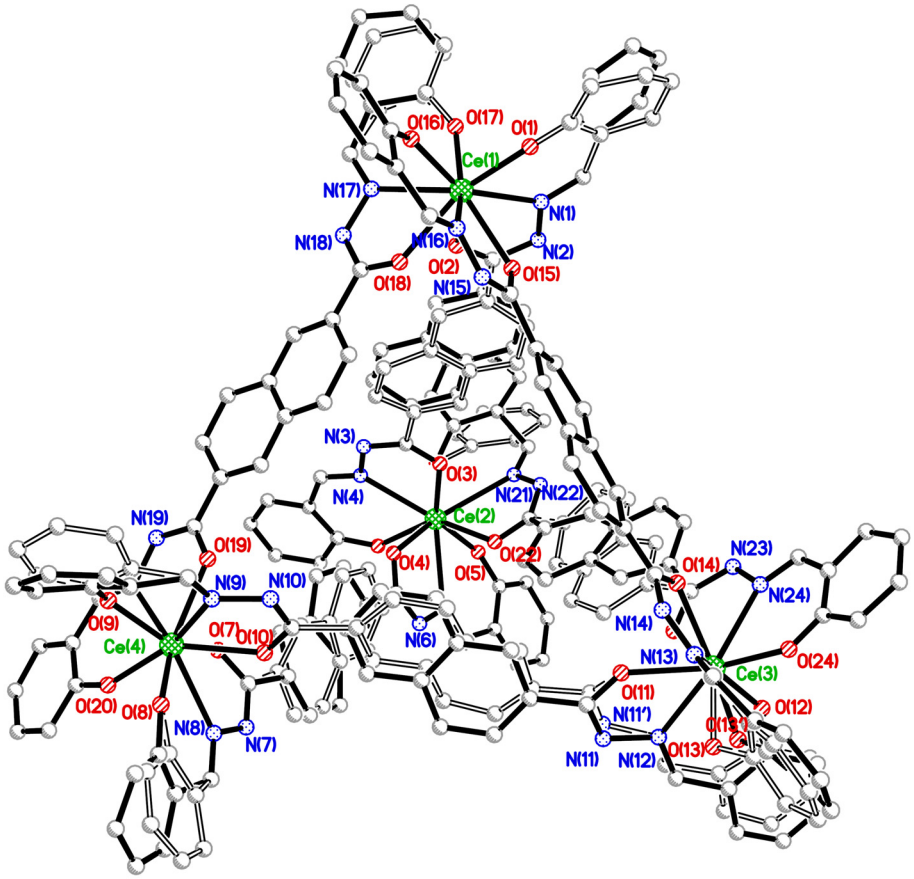

5. Figure S3 The coordination configuration of the Ce(1) centre in **TE1**. The bond lengthes (Å) and angles (°) of the Ce(1) centre: Ce(1)–O(1) 2.229(3), Ce(1)–O(2) 2.414(4), Ce(1)–O(15) 2.412(4), Ce(1)–O(16) 2.224(4), Ce(1)–O(17) 2.212(4), Ce(1)–O(18) 2.448(4), Ce(1)–N(1) 2.595(5), Ce(1)–N(16) 2.607(5), Ce(1)–N(17) 2.687(4); O(17)–Ce(1)–O(16) 84.6(2), O(17)–Ce(1)–O(1) 86.6(2), O(16)–Ce(1)–O(1) 85.5(1), O(17)–Ce(1)–O(2) 86.0(2), O(16)–Ce(1)–O(2) 141.8(1), O(1)–Ce(1)–O(2), 130.5(1), O(17)– Ce(1)–O(15) 143.8(2), O(16)–Ce(1)–O(15) 130.1(2), O(1)–Ce(1)–O(15) 83.8(1), O(2)–Ce(1)–O(15) 74.3(1), O(17)–Ce(1)–O(18) 129.7(2), O(16)–Ce(1)–O(18) 88.4(1), O(1)–Ce(1)–O(18) 142.2(1), O(2)–Ce(1)–O(18) 70.6(1), O(15)–Ce(1)–O(18) 72.1(1), O(17)–Ce(1)–N(1) 76.1(2), O(16)–Ce(1)– N(1) 148.2(2), O(1)–Ce(1)–N(1) 69.3(2), O(2)–Ce(1)–N(1) 61.4(1), O(15)–Ce(1)–N(1) 67.8(2), O(18)–Ce(1)–N(1) 123.4(2), O(17)–Ce(1)–N(16) 150.2(2), O(16)–Ce(1)–N(16) 68.8(2), O(1)–Ce(1)–N(16) 80.5(2), O(2)–Ce(1)–N(16) 122.6(2), O(15)–Ce(1)–N(16) 61.4(2), O(18)–Ce(1)–N(16) 62.6(1), N(1)–Ce(1)–N(16) 122.9(2), O(17)–Ce(1)–N(17) 67.1(1), O(16)–Ce(1)–N(17) 76.1(1), O(1)–Ce(1)–N(17) 149.2(2), O(2)–Ce(1)–N(17) 65.9(1), O(15)–Ce(1)–N(17) 127.0(1), O(18)–Ce(1)– N(17) 62.7(1), N(1)–Ce(1)–N17 116.4(2), N(16)–Ce(1)–N(17) 114.3(1).

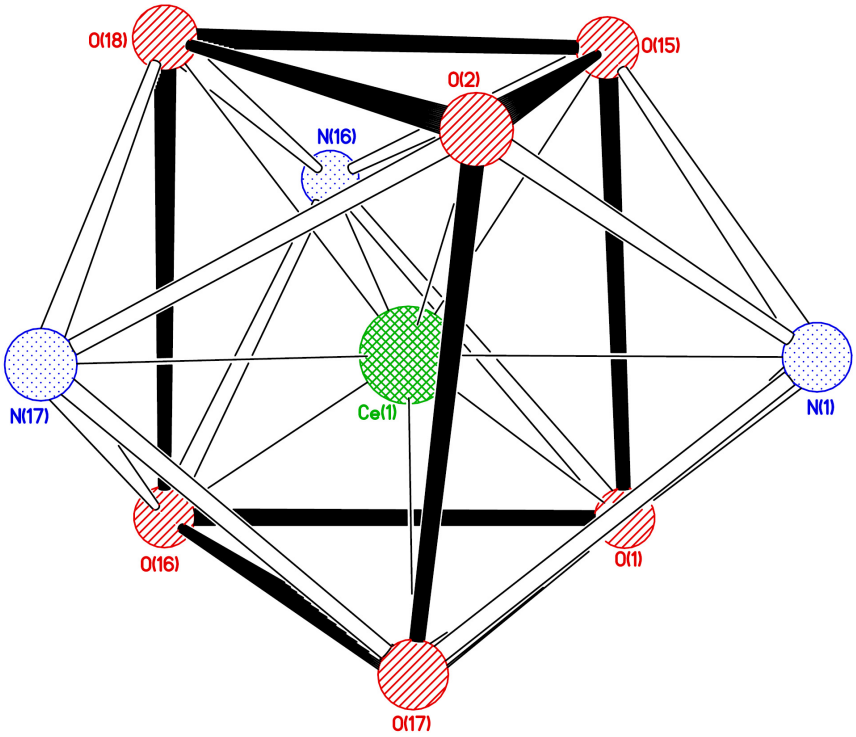

6. Figure S4 The coordination configuration of the Ce(2) centre in **TE1**. The bond lengthes (Å) and angles (°) of the Ce(2) centre: Ce(2)–O(3) 2.317(4), Ce(2)–O(4) 2.230(4), Ce(2)–O(5) 2.187(3), Ce(2)–O(6) 2.445(4), Ce(2)–O(21) 2.167(4), Ce(2)–O(22) 2.491(4), Ce(2)–N(4) 2.594(5), Ce(2)–N(5) 2.674(5), Ce(2)–N(21) 2.614(5); O(21)–Ce(2)– O(5) 84.6(2), O(21)–Ce(2)–O(4) 87.0(2), O(5)–Ce(2)–O(4) 85.5(1), O(21)–Ce(2)–O(3) 85.9(2), O(5)–Ce(2)–O(3) 140.0(1), O(4)–Ce(2)–O(3) 132.8(1), O(21)– Ce(2)–O(6) 143.5(2), O(5)–Ce(2)–O(6) 129.2(1), O(4)–Ce(2)–O(6) 83.5(1), O(3)–Ce(2)–O(6) 75.4(1), O(21)–Ce(2)–O(22) 128.7(1), O(5)–Ce(2)–O(22) 87.1(1), O(4)–Ce(2)–O(22) 142.6(1), O(3)–Ce(2)–O(22) 69.2(1), O(6)–Ce(2)–O(22) 73.3(1), O(21)–Ce(2)–N(4) 77.1(2), O(5)–Ce(2)–N(4) 150.8(2), O(4)–Ce(2)–N(4) 71.2(2), O(3)–Ce(2)–N(4) 61.7(1), O(6)–Ce(2)–N4 66.5(2), O(22)–Ce(2) –N(4) 122.1(2), O(21)–Ce(2)–N(21) 69.7(1), O(5)–Ce(2)–N(21) 75.5(1), O(4)–Ce(2)–N(21) 150.8(2), O(3)–Ce(2)–N(21) 64.8(1), O(6)–Ce(2)–N(21) 125.7(1), O(22)–Ce(2)–N(21) 59.2(1), N(4)–Ce(2)–N(21) 117.8(2), O(21)–Ce(2)– N(5) 150.6(2), O(5)–Ce(2)–N(5) 69.0(2), O(4)–Ce(2)–N(5) 78.3(2), O(3)–Ce(2)–N(5) 122.7(2), O(6)–Ce(2)–N(5) 60.2(1), O(22)–Ce(2)–N(5) 64.8(1), N(4)–Ce(2)–N(5) 120.5(2), N(21)–Ce(2)–N(5) 113.7(2).

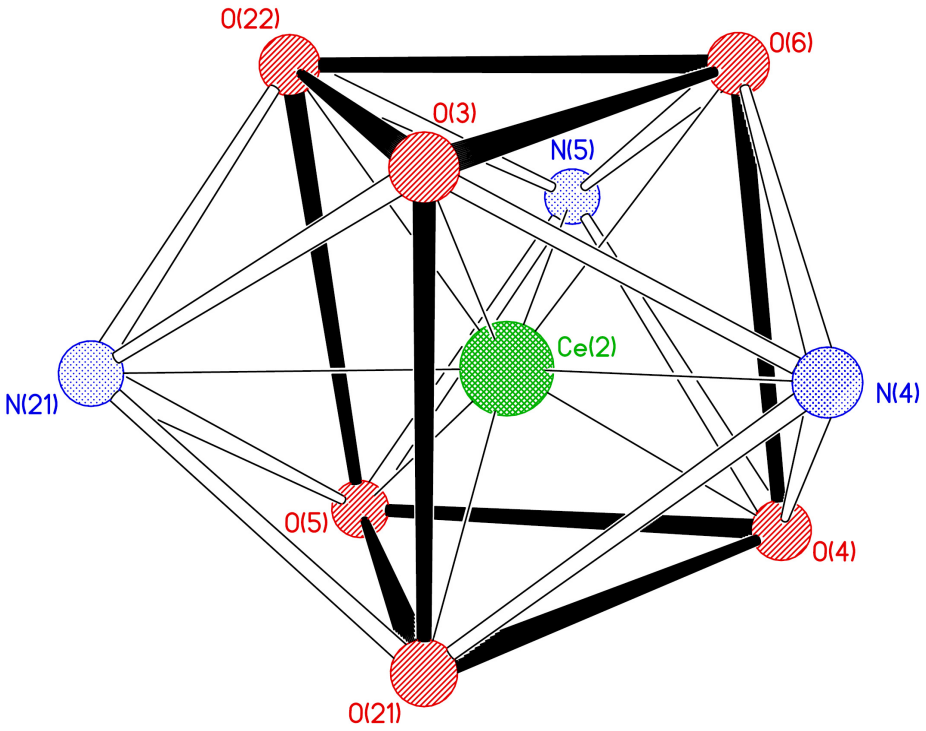

7. **Figure S5** The coordination configuration of the Ce(3) centre in **TE1**, the disordered O(13') atom was omitted. The bond lengthes and angles of the Ce(3) centre: Ce(3)–O(11) 2.357(4), Ce(3)–O(12) 2.221(5), Ce(3)–O(13) 2.126(8), Ce(3)–O(13') 2.335(8), Ce(3)–O(14) 2.437(4), Ce(3)–O(23) 2.374(4), Ce(3)– O(24) 2.160(3), Ce(3)–N(12) 2.612(6), Ce(3)–N(13) 2.561(6), Ce(3)–N(24) 2.644(5); O(24)–Ce(3)– O(13) 87.7(2), O(24)–Ce(3)–O(12) 85.0(2), O(13)–Ce(3)–O(12) 77.3(3), O(24)–Ce(3)–O(13') 76.8(2), O(12)–Ce(3)–O(13') 89.1(2), O(24)–Ce(3)–O(11) 140.7(2), O(13)–Ce(3)–O(11) 88.1(3), O(12)– Ce(3)–O(11) 131.8(2), O(13')–Ce(3)–O(11) 88.8(2), O(24)–Ce(3)–O(23) 129.9(2), O(13)–Ce(3)– O(23) 135.8(2), O(12)–Ce(3)–O(23) 83.3(2), O(13')–Ce(3)–O(23) 151.0(2), O(11)–Ce(3)–O(23) 75.9(2), O(24)–Ce(3)–O(14) 89.2(2), O(13)–Ce(3)–O(14) 136.0(6), O(12)–Ce(3)–O(14) 146.0(1), O(13')–Ce(3)–O(14) 122.0(2), O(11)–Ce(3)–O(14) 67.7(2), O(23)–Ce(3)–O(14) 75.0(2), O(24)–Ce(3)–N(13) 73.3(2), O(13)–Ce(3)–N(13) 76.1(3), O(12)–Ce(3)–N(13) 146.0(2), O(13')–Ce(3)–N(13) 61.0(2), O(11)–Ce(3)–N(13) 67.8(2), O(23)–Ce(3)–N(13) 130.6(2), O(14)–Ce(3)–N(13) 61.0(2), O(24)–Ce(3)–N(12) 146.6(2), O(13)–Ce(3)–N(12) 66.6(3), O(12)–Ce(3)–N(12) 69.4(2), O(13')– Ce(3)–N(12) 81.7(2), O(11)–Ce(3)–N(12) 62.7(3), O(23)–Ce(3)–N(12) 69.5(2), O(14)–Ce(3)–N(12) 124.0(2), N(13)–Ce(3)–N(12) 117.3(2), O(24)–Ce(3)–N(24) 65.5(2), O(13)–Ce(3)–N(24) 147.7(2), O(12)–Ce(3)–N(24) 82.6(2), O(13')–Ce(3)–N(24) 141.8(2), O(11)–Ce(3)–N(24) 122.9(2), O(23)– Ce(3)–N(24) 64.8(1), O(14)–Ce(3)–N(24) 64.7(2), N(13)–Ce(3)–N(24) 110.2(2), N(12)–Ce(3)–N(24) 128.4(2).

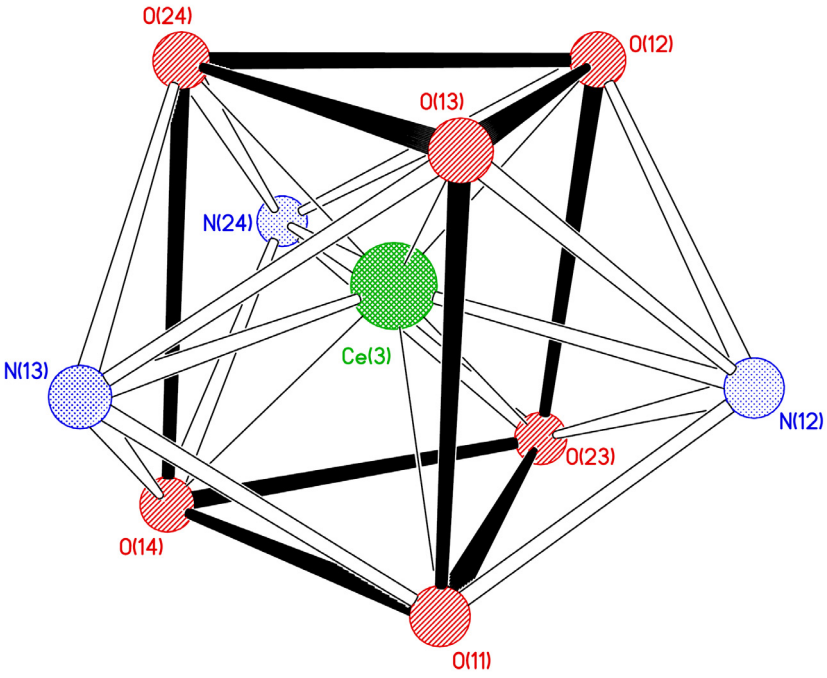

8. Figure S6 The coordination configuration of the Ce(4) centre in **TE1**. The bond lengthes and angles of the Ce(4) centre: Ce(4)–O(8) 2.159(4), Ce(4)–O(20) 2.189(3), Ce(4)–O(9) 2.238(4), Ce(4)–O(10) 2.379(4), Ce(4)–O(19) 2.395(4), Ce(4)–O(7) 2.481(4), Ce(4)–N(8) 2.622(5), Ce(4)–N(20) 2.656(5), Ce(4)–N(9) 2.660(5); O(8)–Ce(4)–O(20) 85.4(2), O(8)–Ce(4)–O(9) 84.6(2), O(20)–Ce(4)–O(9) 88.0(1), O(8)–Ce(4)–O(10) 88.1(2), O(20)–Ce(4)–O(10) 139.3(2), O(9)–Ce(4)–O(10) 131.3(1), O(8)–Ce(4)–O(19) 142.1(2), O(20)–Ce(4)–O(19) 129.6(1), O(9)–Ce(4)–O(19) 83.2(2), O(10)–Ce(4)– O(19) 73.8(1), O(8)–Ce(4)–O(7) 129.5(2), O(20)–Ce(4)–O(7) 84.4(1), O(9)–Ce(4)–O(7) 144.1(1), O(10)–Ce(4)–O(7) 69.2(1), O(19)–Ce(4)–O(7) 75.2(1), O(8)–Ce(4)–N(8) 68.4(2), O(20)–Ce(4)–N(8) 76.2(2), O(9)–Ce(4)–N(8) 149.5(2), O(10)–Ce(4)–N(8) 64.1(2), O(19)–Ce(4)–N(8) 127.0(2), O(7)–Ce(4)–N(8) 61.0(1), O(8)–Ce(4)–N(20) 149.7(1), O(20)–Ce(4)–N(20) 68.5(1), O(9)–Ce(4)–N(20) 79.5(1), O(10)–Ce(4)–N(20) 121.6(1), O(19)–Ce(4)–N(20) 61.2(1), O(7)–Ce(4)–N(20) 65.0(1), N(8)–Ce(4)–N(20) 117.0(2), O(8)–Ce(4)–N(9) 76.6(2), O(20)–Ce(4)–N(9) 151.4(2), O(9)–Ce(4)– N(9) 68.5(1), O(10)–Ce(4)–N(9) 63.0(1), O(19)–Ce(4)–N(9) 65.5(1), O(7)–Ce(4)–N(9) 124.2(1), N(8)–Ce(4)–N(9) 116.2(2), N(20)–Ce(4)–N(9) 120.0(2).

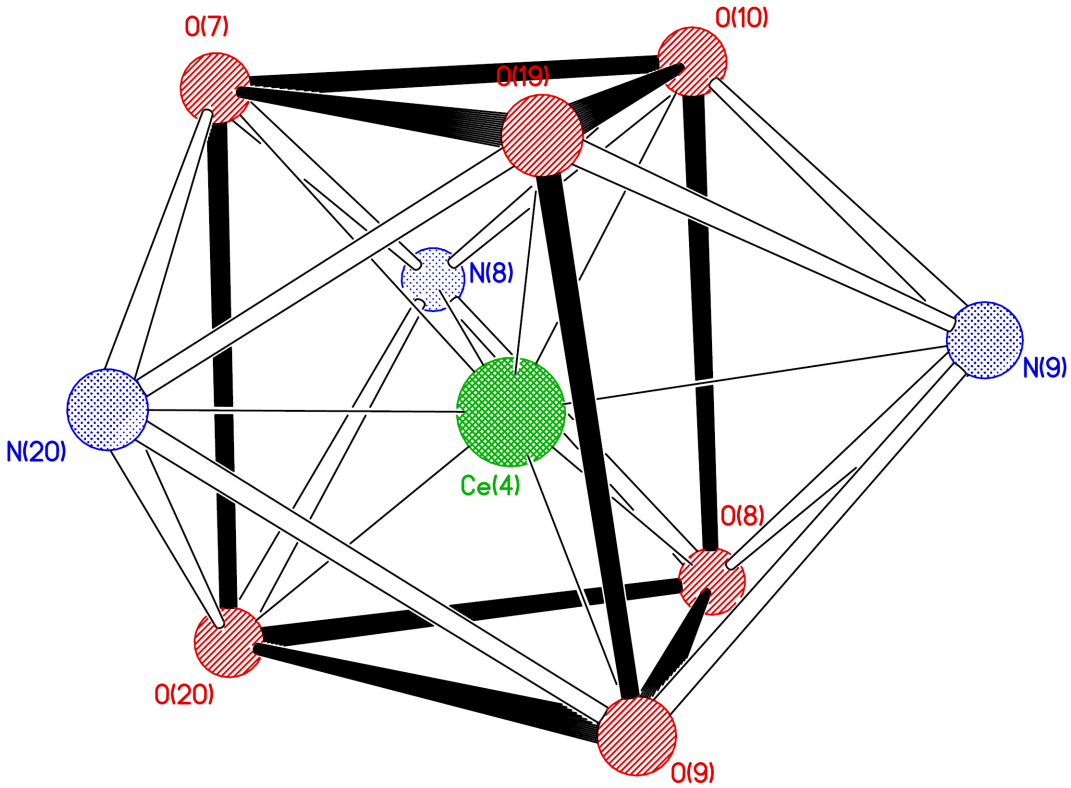

9. Figure S7 Plot of $\chi_M T$ *vs.* T per tetrahedron for a polycrystalline sample of compound **TE1**.

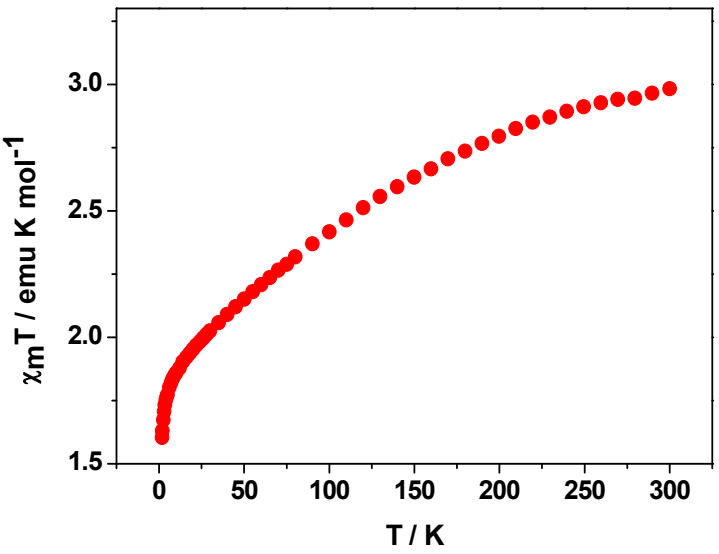

10. Figure S8.1 The Uv-*vis* absorption spectra of $\mathbf{H_2L^1}$ (red line), **TE1** (black line) in DMF/acetonitrile solution (15:85, v/v). For a comparison, here the molar absorptivity of **TE1** is calculated as one sixth of the value of itself, corresponding to the number of ligands in the complex. .

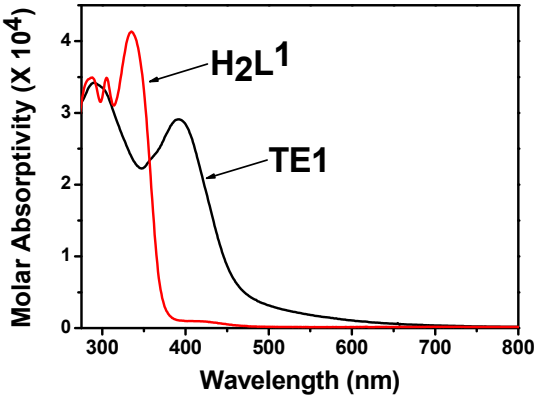

Figure S8.2 The family of the Uv-*vis* absorption spectra of $\mathbf{H_2L^2}$ (red line), **TE2**(black line). For a comparison, here the molar absorptivity of **TE2** is calculated as one sixth of the value of itself, corresponding to the number of ligands in the complex.

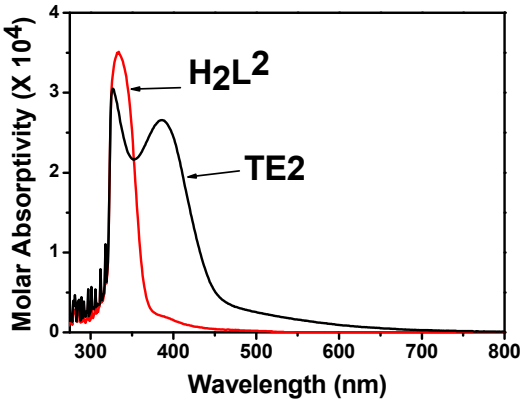

11. Figure S9.1 Fluorescent spectrum of ligand $\mathbf{H_2L^1}$ (50 μM, red line) and complex **TE1** (50 μM, black line) in DMF/acetonitrile solution (15:85, v/v), excited at 360 nm..

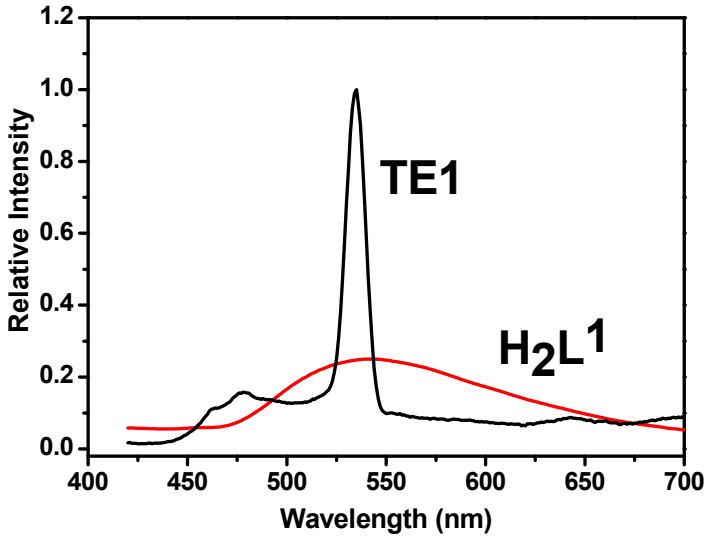

Figure S9.2 Fluorescent response of ligand $\mathbf{H_2L^2}$ (50 μM, red line) and complex **TE2** (50 μM, black line) in DMF/acetone solution (5:95, v/v), excited at 320 nm.

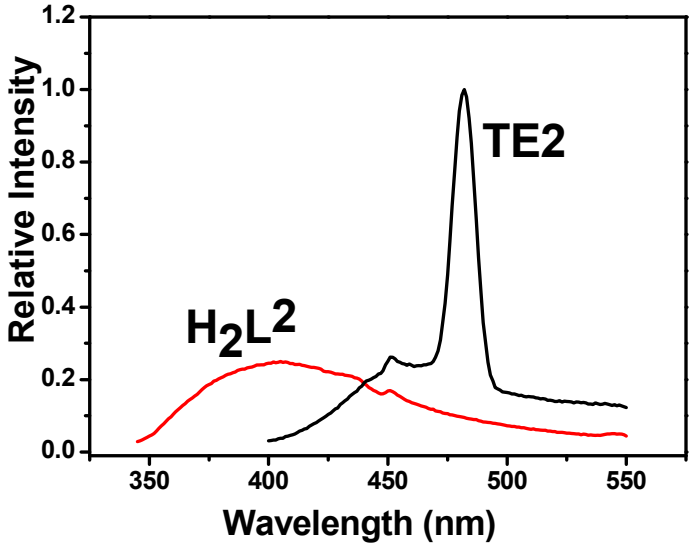

12. Figure S10 Family of Uv-*vis* absorption spectra of **TE1** in DMF/acetonitrile solution (15:85, v/v, 4 μM) upon the addition of various monosaccharides and disaccharides.

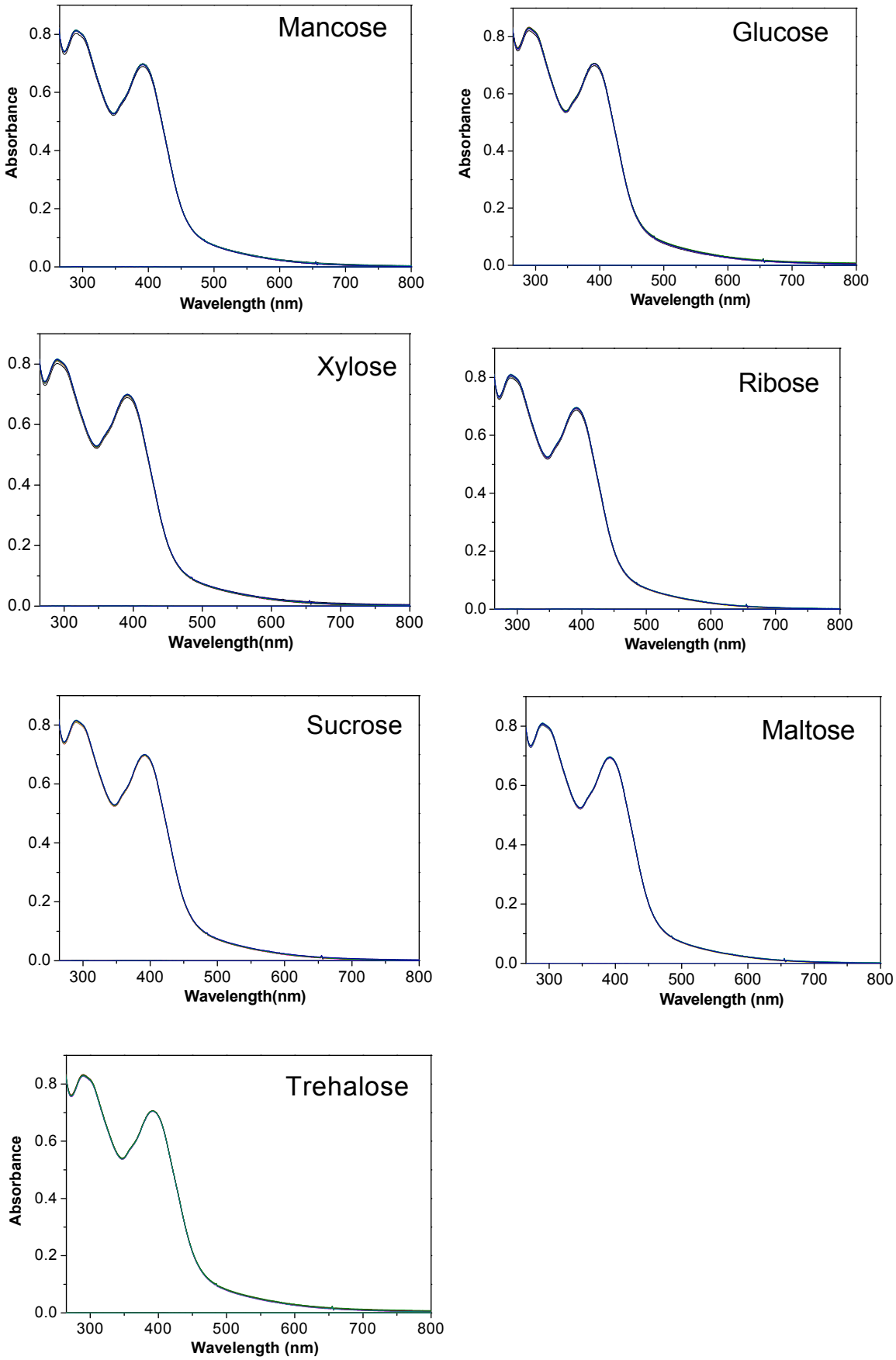

13. Figure S11 Family of fluorescent spectra of **TE1** in DMF/acetonitrile solution (15:85, v/v, 50μM) upon the addition of various monosaccharides and disaccharides, excited at 360 nm.

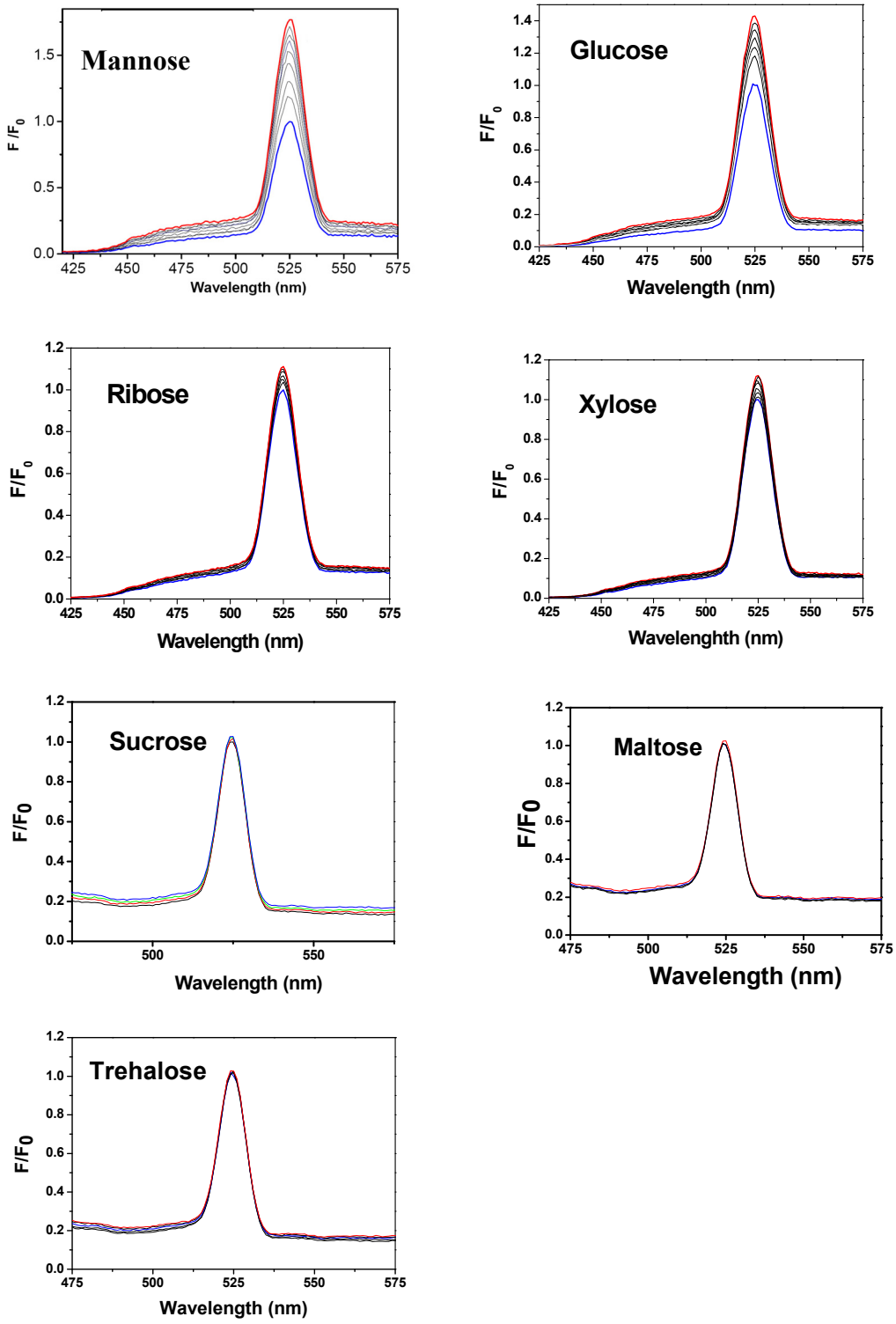

14. Figure S12 Family of Uv-*vis* absorption spectra of **TE2** (4 μM**)** in DMF/acetone solution (5:95, v/v) upon the addition of various monosaccharides and disaccharides.

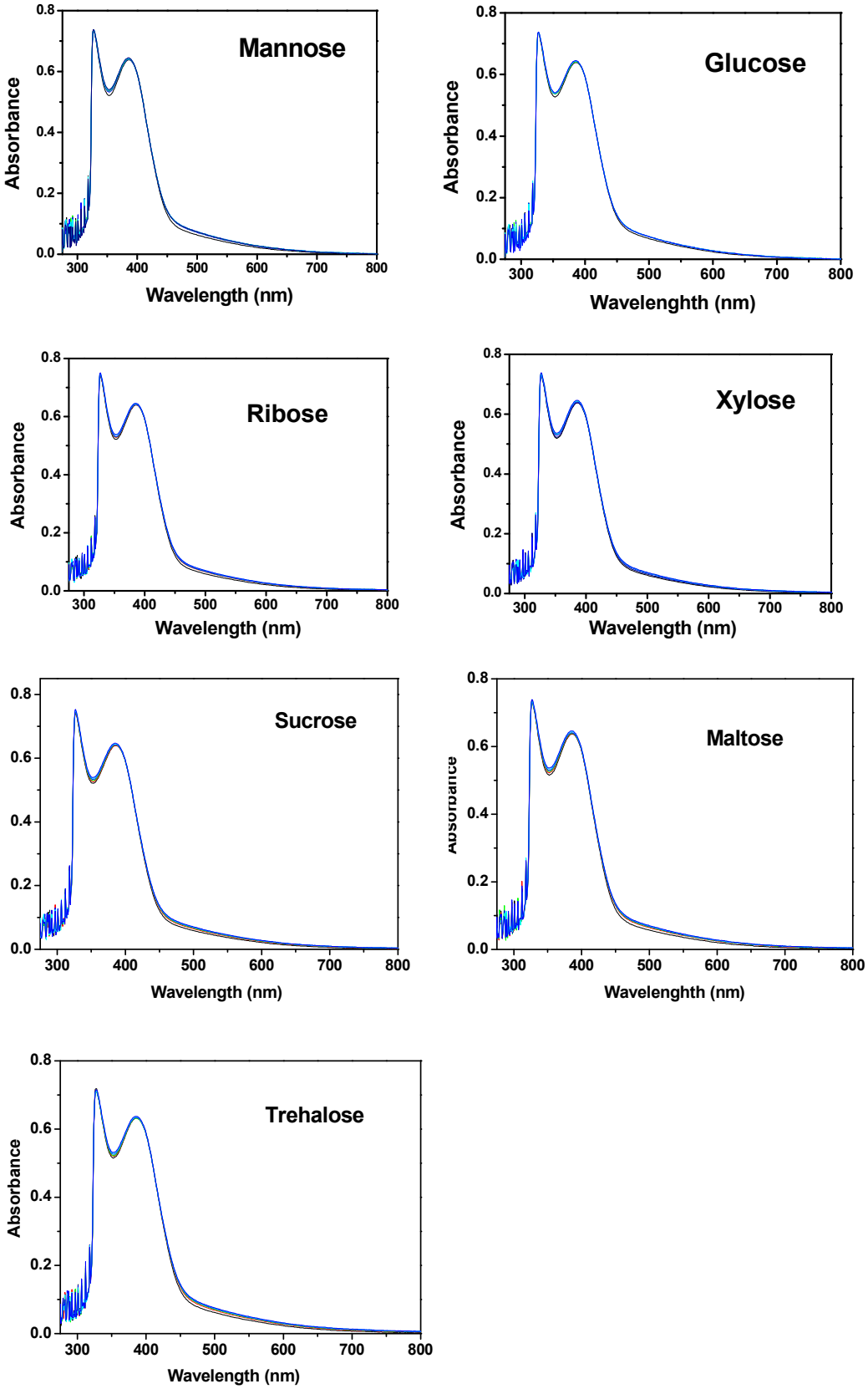

15. Figure S13 Family of fluorescent spectra of **TE2** in DMF/acetone solution (5:95, v/v, 20μM) upon the addition of various monosaccharides and disaccharides, excited at 320 nm.

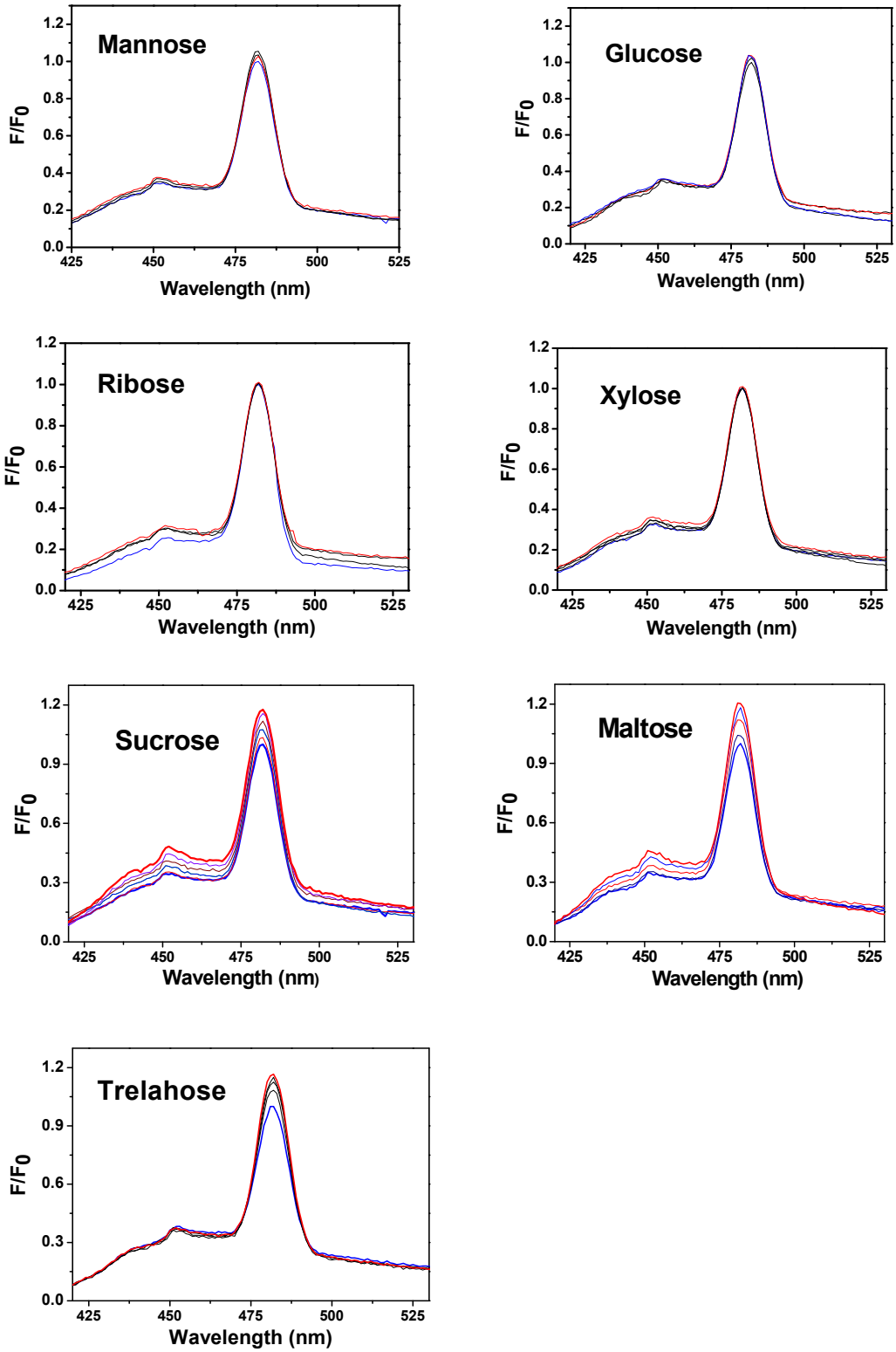

16. Figure S14 Linear fit for log[$(F–F_0)/ (F_L–F)$] *vs.* log[G] for corresponding titration curve of **TE2**.

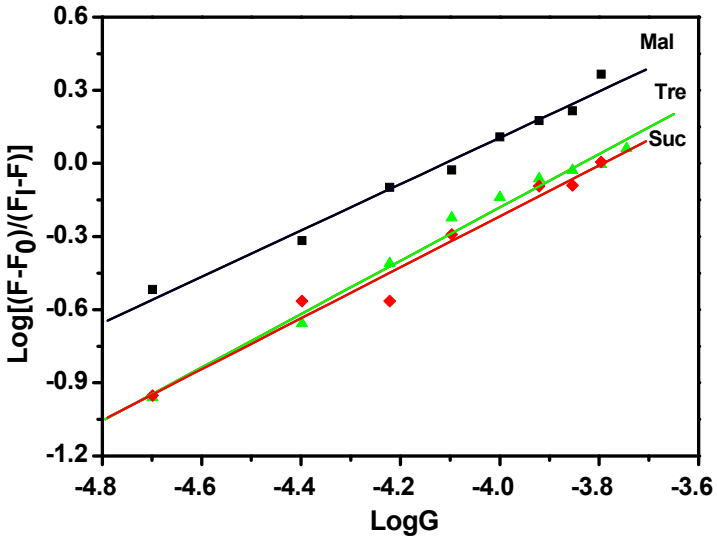

17. Figure S15 XRD pattern of compound **TE1** data (bottom) and simulation of the XRD according to single crystal diffraction of **TE1** (top).